Random matrix theory and higher genus integrability: the quantum chiral Potts model

J-Ch Anglès d'Auriac[1]**, J-M Maillard**[2] **and C M Viallet**[2]

[1] Centre de Recherches sur les Très Basses Températures, BP 166, 38042 Grenoble, France
[2] LPTHE, Tour 16, 1er étage, Boîte 126, 4 Place Jussieu, 75252 Paris Cedex 05, France

E-mail: dauriac@polycnrs-gre.fr, maillard@lpthe.jussieu.fr and viallet@lpthe.jussieu.fr

Abstract
We perform a random matrix theory (RMT) analysis of the quantum four-state chiral Potts chain for different sizes of the chain up to size $L = 8$. Our analysis gives clear evidence of a Gaussian orthogonal ensemble (GOE) statistics, suggesting the existence of a generalized time-reversal invariance. Furthermore, a change from the (generic) GOE distribution to a Poisson distribution occurs when the integrability conditions are met. The chiral Potts model is known to correspond to a (star-triangle) integrability associated with curves of genus higher than zero or one. Therefore, the RMT analysis can also be seen as a detector of 'higher genus integrability'.

PACS numbers: 05.50.+q, 05.20.−y, 05.45.+b

Introduction

Initially developed in the framework of nuclear or atomic physics [1], random matrix theory (RMT) provides a versatile characterization of chaos [2]. Since the pioneering work of Wigner [3], Dyson [4] and Mehta [5], RMT has been applied successfully to various domains of physics. As a limiting case RMT signals the emergence of integrability, which shows up in the change of the generic Wignerian level spacing distribution into Poissonian or Dirac distributions. The first examples of this appeared when considering simple harmonic oscillators (totally rigid spectrum) or free fermion models [6–8]. The reduction to Poisson distribution reflects nothing but the independence of the eigenvalues. This change in the distribution may sometimes come from a dimensional reduction of the model, as in the so-called disorder solutions [9–11]. It can also be found in genuinely correlated systems, the reduction being now associated with the Bethe ansatz integrability [12–15] or Yang–Baxter integrability [16] with rational or elliptic functions. It is natural to ask whether this link between Poisson reduction and Yang–Baxter integrability still holds when the solutions of the Yang–Baxter equations *are no longer parametrized in terms of Abelian varieties*. The perfect

example to address this question is the chiral Potts model for which Au-Yang *et al* found a higher genus solution [17] of the Yang–Baxter equations. These solutions appeared in the two-dimensional *classical* chiral Potts model on an anisotropic square lattice (see for instance [18]). As a consequence of the Yang–Baxter equations, there exists a family of commuting transfer matrices, also commuting with some quantum Hamiltonian given below for the chiral Potts model (see (1) in the following section). The RMT approach can be applied directly to analyse the eigenvalues of the transfer matrices of the two-dimensional classical models [9], but of course it is much simpler when applied to quantum Hamiltonians, since the latter[3] does not depend on the spectral parameters. It is also numerically much more convenient. For the sake of simplicity we restrict ourself to the RMT analysis of the quantum Hamiltonian.

The paper is organized as follows. In section 1 we recall some results of the chiral Potts model. In section 2 we review how to use, in practice, RMT in the context of quantum Hamiltonian. In section 3 we review some symmetries of the quantum Hamiltonian of the chiral Potts model, and discuss time-reversal invariance. Our numerical results are presented in section 4, where we also discuss the unexpected occurrence of a GOE statistics.

1. The quantum chiral Potts chain

The Hamiltonian of the quantum chiral Potts chain first introduced by Howes *et al* [19] and von Gehlen and Rittenberg [20] is defined by

$$H \equiv H_X + H_{ZZ} = \sum_j H_{jj+1} = -\sum_j \sum_{n=1}^{N-1} \left[\overline{\alpha_n} \cdot (X_j)^n + \alpha_n \cdot (Z_j Z_{j+1}^\dagger)^n \right] \quad (1)$$

where $X_j = I_N \otimes \cdots \otimes X \otimes \cdots \otimes I_N$ and $Z_j = I_N \otimes \cdots \otimes Z \otimes \cdots \otimes I_N$. Here I_N is an $N \times N$ unit matrix while X and Z are $N \times N$ matrices, in jth position in the tensor product, with the following entries:

$$Z_{j,m} = \delta_{j,m} \exp[2\pi \mathrm{i}(j-1)/N] \quad \text{and} \quad X_{j,m} = \delta_{j,m+1} (\mathrm{mod}\ N).$$

The self-dual model [21] corresponds to $\alpha_n = \overline{\alpha_n}$. Conformal theory analysis of the three-state model can be found in [22]. Some spectral analyses of this model have been performed for the quantum self-dual model or the three-state model [20, 23, 24].

In this paper we restrict ourself to the $N = 4$ (four-state chiral Potts model) non-self-dual case. The integrability conditions read (see equations (33a), (33b), (33c) and (33d) in [18])

$$\frac{\overline{\alpha_2}^2}{\overline{\alpha_1 \alpha_3}} = \frac{\alpha_2^2}{\alpha_1 \alpha_3} \quad (2)$$

$$\frac{\overline{\alpha_1}^2 + \overline{\alpha_3}^2}{\overline{\alpha_2}} = \frac{\alpha_1^2 + \alpha_3^2}{\alpha_2} \quad (3)$$

$$\left(\alpha_1^2 - \alpha_3^2\right)\left(2\alpha_2^2 - \alpha_1 \alpha_3\right) = 0 \quad (4)$$

$$\left(\overline{\alpha_1}^2 - \overline{\alpha_3}^2\right)\left(2\overline{\alpha_2}^2 - \overline{\alpha_1 \alpha_3}\right) = 0. \quad (5)$$

There are several simple solutions such as (up to a multiplicative common factor)

$$(\alpha_1, \alpha_2, \alpha_3, \overline{\alpha_1}, \overline{\alpha_2}, \overline{\alpha_3}) = (r, 1, r, \pm r, 1, \pm r) \quad \text{or}$$

$$= (r, 1, r, \pm \mathrm{i} \cdot r, -1, -\pm \mathrm{i} \cdot r). \quad (6)$$

---

[3] The fact that the Hamiltonian does not depend on the spectral parameters does not necessarily mean that it is blind to the Abelian or non-Abelian character of the integrability varieties. This appears when one tries to build the eigenvectors of the quantum Hamiltonian of the quantum chiral Potts chain, via the Bethe ansatz, since the method fails for higher genus spectral curves.

One of these solutions is a self-dual solution and the others are also quite trivial. In the last two equations (4) and (5), we choose the second factor of the left-hand side to be zero.

In order to have a real spectrum we choose $\alpha_1 = \alpha_3^\star$, $\alpha_2 = \alpha_2^\star$, $\overline{\alpha_2} = \overline{\alpha_2}^\star$ and $\overline{\alpha_1} = \overline{\alpha_3}^\star$ (where the star denotes the complex conjugate) yielding a hermitian Hamiltonian. A possible parametrization is then

$$
\begin{aligned}
\alpha_1 = \alpha_3^\star = \sqrt{1+r} + \mathrm{i}\sqrt{1-r} && \alpha_2 = 1 \\
\overline{\alpha_1} = \overline{\alpha_3}^\star = \sqrt{n^2 + rn} + \mathrm{i}\sqrt{n^2 - rn} && \overline{\alpha_2} = n
\end{aligned}
\tag{7}
$$

where r and n are real and such that $|r| < |n|$ and $|r| < 1$. The value $n = 1$ yields the self-dual situation. Note that we can scale $\alpha_1, \alpha_2, \alpha_3, \overline{\alpha_1}, \overline{\alpha_2}$ and $\overline{\alpha_3}$ by the same common factor which enables us to normalize $\alpha_2 = 1$ in (7).

2. The RMT machinery

Performing an RMT analysis means that one considers the spectrum of the quantum Hamiltonian, or of the transfer matrix, as a collection of numbers, and looks for some possibly universal statistical properties of this collection of numbers. Indeed, neither the raw spectrum, nor the raw level spacing distribution, have any universal property. In order to uncover them, one has to perform some normalization of the spectrum: the so-called *unfolding* operation. This amounts to making the *local* density of eigenvalues of the spectrum equal to unity everywhere [25–28]. In other words, one subtracts the regular part from the integrated density of states and considers only the fluctuations. It is believed that the unfolded spectra of many quantum systems are very close to one of four archetypal situations described by four statistical ensembles emerging from the analysis of the (real) spectrum of random[4] matrices [5]. For integrable models this is the statistical ensemble of diagonal random matrices, while for non-integrable systems this can be the Gaussian orthogonal ensemble (GOE), the Gaussian unitary ensemble (GUE), or the Gaussian symplectic ensemble (GSE), depending on the symmetries of the model under consideration. One-dimensional quantum systems, for which the Bethe ansatz works, have a level spacing distribution close to a Poissonian (exponential) distribution [30], $P(s) = \exp(-s)$, whereas if the Bethe ansatz does not work, the level spacing distribution can be approximated, if the Hamiltonian is time-reversal invariant, either by the Wigner surmise for the Gaussian orthogonal ensemble (GOE):

$$
P_{\mathrm{GOE}}(s) \simeq \frac{\pi}{2} s \exp(-\pi s^2/4)
\tag{8}
$$

or by the Gaussian symplectic ensemble (GSE):

$$
P_{\mathrm{GSE}}(s) \simeq B^3 s^4 \exp(-Bs^2)
\tag{9}
$$

where $B = \left(\frac{8}{3}\right)^2 \frac{1}{\pi} \simeq 2.263$. Note that GOE can also occur in a slightly more general framework ('false' time-reversal violation, A-adapted basis [31]). When one does not have any time-reversal symmetry, the Gaussian unitary ensemble distribution should appear as

$$
P_{\mathrm{GUE}}(s) \simeq \frac{32}{\pi^2} s^2 \exp(-4s^2/\pi).
\tag{10}
$$

The above three expressions are good approximations of the exact $P(s)$, the latter being solutions of particular Painlevé equations [32–36].

---

[4] By random matrices one means that the entries of the matrices are *independent Gaussian random variables*. This is a crucial assumption. Of course, if the entries are not independent Gaussian random variables, one can get all kinds of cross-overs between these four statistical ensembles [29].

Two-dimensional quantum spin systems were numerically shown to yield the GOE distribution [25, 37, 38]. Other statistical properties may also be studied, such as correlations between eigenvalues (see section 2.2), but the core of the analysis will be to compare the level spacing distribution of the unfolded spectrum with the Poisson and the three Gaussian distributions.

2.1. The unfolding procedure

The unfolding can be achieved by different means [28]. There is however no rigorous prescription and the best criterion is the insensitivity of the final result to the method employed and/or to the parameters which any unfolding method introduces, for reasonable variation. We denote by E_i the raw eigenvalues and by ϵ_i the corresponding 'unfolded' eigenvalues. The unfolding requirement is that the local density of the ϵ_is is equal to one. One needs to compute an averaged integrated density of states $\bar{\rho}(E)$ from the actual integrated density of states:

$$\rho(E) = \frac{1}{N} \int_{-\infty}^{E} \sum_i \delta(e - E_i) \, \mathrm{d}e$$

and then we take $\epsilon_i = N\bar{\rho}(E_i)$. In order to compute $\bar{\rho}(E)$ from $\rho(E)$, several methods are possible. One can choose a suitable odd integer $2r + 1$ of the order of 9–25 and then replace each eigenvalue E_i by a local average:

$$E_i' = \frac{1}{2r + 1} \sum_{j=i-r}^{i+r} E_j. \tag{11}$$

Then $\bar{\rho}(E)$ is approximated by the linear interpolation between the points of coordinates (E_i', i). Another method consists in replacing each delta peak in $\rho(E)$ by a Gaussian distribution centred at the location of the peak and with a properly chosen mean square deviation. There are two ways to choose this variance: one can set the same mean square deviation for every peak, or even better, one chooses a different mean square deviation for each peak, so that the number of neighbouring peaks inside half-width of the Gaussian distribution is kept constant. Another method is to discard the low frequency components in a Fourier transform of $\rho(E)$. A detailed explanation and tests of these methods of unfolding are given in [39]. Note that all these methods require an adjustment parameter (the number r defining the running average, the mean square deviation itself or the number of neighbouring peaks inside the half-width for Gaussian unfolding, the cut-off for Fourier unfolding). When this adjustment parameter is large, the smoothing becomes too efficient, and the fluctuations are washed out. By contrast too small an adjustment parameter gives a totally rigid level spacing: the unfolded integrated density of states coincides with the raw integrated density of states. Out of the three methods, the moving average unfolding is the fastest one, but the Gaussian with adapted mean square deviation gives the best results. Notice that extremal eigenvalues are discarded since they are affected by finite size effects and this introduces another, slightly less pertinent, adjustment parameter.

2.2. Quantities characterizing the spectrum

Once the spectrum has been computed, sorted and unfolded, various statistical properties of the spectrum can be investigated. The simplest one, which is also the most significant and the most universal, is the distribution $P(s)$ of level spacings $s = \epsilon_{i+1} - \epsilon_i$ between two consecutive unfolded eigenvalues ϵ_i and ϵ_{i+1}. The distribution $P(s)$ will be compared to an

exponential distribution and to the GOE Wigner law (8). Usually, a simple visual inspection is sufficient to recognize the presence of *level repulsion* [1], the main property for non-integrable models. In order to quantify the degree of level repulsion, it is convenient to use a parametrized distribution which interpolates between the Poisson law and the GOE Wigner law. From the many possible distributions, we have chosen the *Brody distribution*:

$$P_\beta(s) = c_1 s^\beta \exp\left(-c_2 s^{\beta+1}\right) \tag{12}$$

with

$$c_2 = \left[\Gamma\left(\frac{\beta+2}{\beta+1}\right)\right]^{1+\beta} \quad \text{and} \quad c_1 = (1+\beta)c_2. \tag{13}$$

This distribution turns out to be convenient since its indefinite integral can be expressed with elementary functions. It has been widely used in the literature. For $\beta = 0$, this is a simple exponential for the Poisson ensemble, and for $\beta = 1$, one recovers the Wigner distribution for the GOE. Minimizing the quantity

$$\phi(\beta) = \int_0^\infty (P_\beta(s) - P(s))^2 \, \mathrm{d}s \tag{14}$$

yields a value of β which characterizes the magnitude of level repulsion of the distribution $P(s)$. We have always found $\phi(\beta)$ small. When $-0.1 < \beta < 0.2$, the distribution is close to a Poisson law, while for $0.5 < \beta < 1.2$ the distribution is close to the Wigner distribution.

If a distribution is close to the Wigner distribution (respectively the Poisson law), this means that the GOE (respectively the diagonal matrices ensemble) correctly describes the unfolded spectrum, but only at the level of neighbouring eigenvalues. If one wants to go a step further in the description of the spectrum (at a less universal level), it is of interest to compute functions involving higher order correlations such as, for example, the spectral rigidity [5]

$$\Delta_3(E) = \left\langle \frac{1}{E} \min_{a,b} \int_{\alpha-E/2}^{\alpha+E/2} (N(\epsilon) - a\epsilon - b)^2 \, \mathrm{d}\epsilon \right\rangle_\alpha \tag{15}$$

where $\langle \cdots \rangle_\alpha$ denotes averaging over the whole spectrum. This quantity measures the deviation from equal spacing. For a totally rigid spectrum, such as that of the harmonic oscillator, one has $\Delta_3^{\mathrm{osc}}(E) = 1/12$, for an integrable (Poissonian) system one has $\Delta_3^{\mathrm{Poi}}(E) = E/15$, while for the Gaussian orthogonal ensemble one has $\Delta_3^{\mathrm{GOE}}(E) = \frac{1}{\pi^2}(\log(E) - 0.0687) + \mathcal{O}(E^{-1})$. It has been found that the spectral rigidity of quantum spin systems follows $\Delta_3^{\mathrm{Poi}}(E)$ in the integrable case and $\Delta_3^{\mathrm{GOE}}(E)$ in the non-integrable case. However, in both cases, even though $P(s)$ is in good agreement with RMT, deviations from RMT occur for $\Delta_3(E)$ at some system dependent point E^*. This stems from the fact that the rigidity $\Delta_3(E)$ probes correlations beyond nearest neighbours in contrast to $P(s)$.

3. Symmetry analysis

Some symmetry properties of the chiral Potts model can be found in the literature [40]. We briefly sketch and discuss here the symmetries of the chiral Potts Hamiltonian which we use in our analysis.

3.1. First properties of the Hamiltonian

The Hermiticity conditions of the Hamiltonian (1) are $\alpha_1 = \alpha_3^\star$, $\overline{\alpha_1} = \overline{\alpha_3}^\star$, α_2 and $\overline{\alpha_2}$ real. They are compatible with the parametrization (7).

In this work we concentrate on the *four-state* case, for which the operators X and Z read

$$X = \begin{pmatrix} 0 & 1 & 0 & 0 \\ 0 & 0 & 1 & 0 \\ 0 & 0 & 0 & 1 \\ 1 & 0 & 0 & 0 \end{pmatrix} \quad \text{and} \quad Z = \begin{pmatrix} 1 & 0 & 0 & 0 \\ 0 & i & 0 & 0 \\ 0 & 0 & -1 & 0 \\ 0 & 0 & 0 & -i \end{pmatrix}. \tag{16}$$

Note that

$$XZ = iZX \qquad XZ^3 = -iZ^3 X, \ldots. \tag{17}$$

Let p be the 4×4 (symmetric) matrix

$$p = \frac{1}{2} \begin{pmatrix} 1 & 1 & 1 & 1 \\ 1 & i & -1 & -i \\ 1 & -1 & 1 & -1 \\ 1 & -i & -1 & i \end{pmatrix} \tag{18}$$

related to the Z_4 discrete Fourier transform. Note that p is symmetric and unitary. Let R be the spin reversal $\sigma \to -\sigma$ (mod 4):

$$R = \begin{pmatrix} 1 & 0 & 0 & 0 \\ 0 & 0 & 0 & 1 \\ 0 & 0 & 1 & 0 \\ 0 & 1 & 0 & 0 \end{pmatrix}.$$

One verifies immediately that R is an involution ($R = R^{-1}$), that $R = p^2$, and that the conjugation by R permutes the 4×4 matrices X and X^3 on one side, and matrices Z and Z^3 on the other side, i.e.,

$$R \cdot X \cdot R^{-1} = X^3 \qquad R \cdot Z \cdot R^{-1} = Z^3. \tag{19}$$

Matrices X^2 and Z^2 are invariant by the conjugation by R. We introduce the $4^L \times 4^L$ matrix K_R which is the tensor product of matrix R, L times:

$$K_R = R \otimes R \otimes R \cdots R \otimes R. \tag{20}$$

This matrix is symmetric, real and involutive, and therefore also unitary. One easily verifies, from (19), that K_R *commutes with H*. Let U_p be the unitary matrix:

$$U_p = p \otimes p \otimes p \cdots p \otimes p \qquad K_R = U_p \cdot U_p^t = U_p^2. \tag{21}$$

One may perform the change of basis associated with this unitary matrix U_p and the Hamiltonian (1) becomes

$$H_{ZXX} \equiv H_Z + H_{XX} = -\sum_j \sum_{n=1}^{N-1} \left[\overline{\alpha_n} \cdot (Z_j)^n + \alpha_n \cdot (X_j^\dagger X_{j+1})^n \right] \tag{22}$$

since $pXp^{-1} = Z$ and $pZp^{-1} = X^\dagger = X^3$. Obviously both Hamiltonians (1) and (22) have the same spectrum.

Along these lines one should recall the existence of a *duality* symmetry (see [20, 41] for duality for the classical models) exchanging the operators X_j and $Z_j Z_{j+1}^\dagger$ in (1). The dual Hamiltonian is

$$H_{\text{dual}} \equiv -\sum_j \sum_{n=1}^{N-1} \left[\alpha_n \cdot (X_j)^n + \overline{\alpha_n} \cdot (Z_j Z_{j+1}^\dagger)^n \right] \tag{23}$$

and the duality amounts to permuting the α_n and $\overline{\alpha_n}$ in (1). It is also Hermitian for $\alpha_1 = \alpha_3^\star, \overline{\alpha_1} = \overline{\alpha_3}^\star, \alpha_2$ real and $\overline{\alpha_2}$ real. If one compares the real spectrum of (1) and (23) one finds (this has been checked for $L = 3, 4, 5, 6, 7, 8$) that they have the same real spectrum only on the representations which are the most 'symmetric' with respect to the colour $((c, e) = (0, e)$ see below). This is reminiscent of the situation encountered in [42].

3.2. Representation theory

Eigenstates with different quantum numbers are uncorrelated. It is necessary to compare only eigenvalues of states having the same quantum numbers. This amounts to block-diagonalizing the Hamiltonian (see, for instance, p 1710 in [1]), and this is an *essential requirement of the method*. Due to lattice symmetries, as well as permutation of colours for the chiral four-state Potts model (1), there exists a collection of operators S, acting on the same space as the Hamiltonian H, which are *independent of the parameters α_i and $\overline{\alpha_i}$*, and commute with H: $[H(\alpha_i, \overline{\alpha_i}), S] = 0$. The block-diagonalization is done with the help of the character table of irreducible representations of the symmetry group. Details can be found in [28, 39].

In our case, that is, for Hamiltonian (1) or (22) or even (23), the analysis goes as follows. Matrix X is nothing but the shift operator for the colour. Introduce, for a chain (1) of L sites, the $4^L \times 4^L$ matrix: $S_X = X \otimes X \otimes X \cdots X \otimes X$, which shifts simultaneously all the spins by one. Using (17) one finds that S_X and the Hamiltonian (1) commute. This operator S_X generates the Abelian group Z_4. As far as lattice symmetries are concerned, we assume periodic boundary conditions. We also introduce the lattice shift operator of one lattice spacing S_{latt}. Because of the periodic boundary conditions S_{latt} commutes with Hamiltonian (1). Similarly S_{latt} generates the Abelian group Z_L. Obviously S_X and S_{latt} commute and the total symmetry group is generically the Abelian $Z_L \times Z_4$ group. Note that, because of their chirality, these Hamiltonians do not commute with the mirror symmetry which exchanges site n with site $L + 1 - n$. Therefore, the space symmetry group is not the dihedral symmetry group D_L. However, if some additional conditions on the parameters $\alpha_n, \overline{\alpha_n}$ are verified, the symmetry group D_L can reappear.

- The Hamiltonian H_X is Hermitian iff $\overline{\alpha_1} = \overline{\alpha_3}^\star$ and $\overline{\alpha_2} = \overline{\alpha_2}^\star$. The lattice space symmetry group of H_X is always the dihedral group D_L, and its spin symmetry group is generically (i.e. for $\overline{\alpha_1} \neq \overline{\alpha_3}$) the group Z_4, and becomes the dihedral group D_4 when $\overline{\alpha_1} = \overline{\alpha_3}$.
- The Hamiltonian H_{ZZ} is Hermitian iff $\alpha_1 = \alpha_3^\star$ and α_2 is real. The lattice space symmetry group of H_{ZZ} is generically the group Z_L, and is the dihedral group D_L when $\alpha_1 = \alpha_3$. The spin symmetry group of H_{ZZ} is always the dihedral group D_4.

For generic r and n in equations (7), the total symmetry group is $Z_L \times Z_4$. We always restrict ourselves to Hermitian Hamiltonians. Consequently the $4L$ blocks are also Hermitian and they have only *real* eigenvalues. The diagonalization is performed using standard methods of linear algebra (contained in the LAPACK library [43]). The projectors used to block diagonalize the Hamiltonian are

$$P_{e,c} = \left(\sum_{n=0}^{L-1} \omega^{en} S_{\text{latt}}^n \right) \otimes \left(\sum_{k=0}^{3} i^{ck} S_X^k \right) \tag{24}$$

with $\omega = \exp(2\pi i / L)$. This formula specifies the notation used in the rest of the paper, the representations being indexed by (e, c) with $0 \leqslant e < L$ and $0 \leqslant c < 4$. Keep in mind that this block diagonalization (24) is valid for (1) or (23). For (22), the generator S_X of the Z_4 group is replaced by another matrix S, similar to S_X, and (24) is modified accordingly. We will denote this unitary transformation by P_{ZXX}.

3.3. Time-reversal invariance and beyond: the origin of GOE statistics

Th existence of a time-reversal invariance of the Hamiltonian changes the generic GUE distribution into another distribution [3–5, 44].

The anti-unitary time-reversal operator can be written as the composition of a unitary operator K with the complex conjugation C:

$$T = K \cdot C. \tag{25}$$

In the standard case K is a tensor product over all sites of the chain of some spin operator (see for instance equations (26.13b) in [44]). In the following we will have to use a more general notion of time-reversal invariance: K will not be necessarily a tensor product. We will only impose that the unitary operator K is a *constant* matrix which should not depend on the parameters of H. For instance, for Hamiltonian (1), K must be independent of the α_n and $\bar{\alpha}_n$.

In appendix A.1 it is shown that the time-reversal invariance of the Hamiltonian H implies that *K must be either a symmetric or an antisymmetric unitary matrix*, together with the following relation between the unitary operator K and the Hermitian Hamiltonian H:

$$H = K \cdot H^* \cdot K^{-1} = K \cdot H^t \cdot K^{-1} \tag{26}$$

or equivalently

$$K \cdot H^t = H \cdot K \tag{27}$$

where H^* and H^t are, respectively, the complex conjugate, and the transpose, of the Hermitian Hamiltonian H.

Consider first the case where K is a *symmetric and unitary matrix*. Any symmetric and unitary K can be written (see for instance p 224 of [5]) as the product of a unitary operator U and its transpose, namely $K = U \cdot U^t$, and thus the time-reversal symmetry equation (26) becomes $U \cdot U^t \cdot H^t = H \cdot U \cdot U^t$ or equivalently

$$(U^{-1}H \cdot U)^t = U^{-1}H \cdot U. \tag{28}$$

In other words, U defines a change of basis bringing H into a symmetric form $H_{(s)} = U^{-1} \cdot H \cdot U$. The Hamiltonian H being Hermitian, $H_{(s)}$ is also Hermitian and is therefore real symmetric. Its level spacing distribution should have a Gaussian orthogonal ensemble statistics if this real symmetric matrix is generic enough.

Consider now the case where relation (27), is verified with an *antisymmetric* unitary matrix K. The order of the matrix is necessarily even, namely $2N$, otherwise the matrix is singular. One can then perform a unitary change of basis $H \to U^{-1}H \cdot U$ where U not only belongs to the N-dimensional symplectic [45] group $Sp(N)$, but is quaternion real [46, 47]. In that case the level spacing distribution will have a Gaussian symplectic ensemble statistics [4, 5].

The time-reversal symmetry is a particular case of invariance of the Hamiltonian under the action of an anti-unitary[5] operator A. It can be shown [31] that, provided the Hamiltonian has a so-called A-adapted basis (which is the case if A is an involution), the system may display a Gaussian orthogonal ensemble rather than the GUE, even if the Hamiltonian has neither time-reversal invariance nor geometric symmetry.

The form of condition (27) does not depend on the representation of the Hamiltonian. Performing a unitary change of basis: $H \to H' = U \cdot H \cdot U^{-1}$, one gets from (27) that

$$H' \cdot K' = K' \cdot (H')^t \qquad \text{with} \quad K' = U \cdot K \cdot U^t \tag{29}$$

where K' is still a symmetric unitary matrix. Notice that K does not transform by conjugation.

---

[5] In this respect we can also recall the work of von Gehlen [48, 49] where a Z_2-symmetry (a Lee–Yang symmetry at zero magnetic field) survives for non-zero magnetic field as an anti-unitary symmetry on a non-Hermitian Hamiltonian.

Let P denote the change of basis which block-diagonalizes the Hamiltonians, and α, β denote the indices of the blocks. H may be represented by the H_α and $K_{\text{block}} = P \cdot K \cdot P^t$ given by its blocks $K_{\alpha,\beta}$. Condition (27) becomes

$$H_\alpha \cdot K_{\alpha,\alpha} = K_{\alpha,\alpha} \cdot H_\alpha^t \quad \text{and} \quad H_\alpha \cdot K_{\alpha,\beta} = K_{\alpha,\beta} \cdot H_\beta^t. \tag{30}$$

Remark. It is crucial that the unitary operator K is a *constant* matrix. Introducing the unitary matrix V diagonalizing a Hermitian operator H, and Δ the diagonal matrix of *real* eigenvalues of H, one sees that

$$V \cdot H \cdot V^{-1} = \Delta = \Delta^* = V^* \cdot H^* \cdot (V^{-1})^* = V^* \cdot H^* \cdot (V^*)^{-1} \quad \text{or}$$
$$H \cdot V^{-1} \cdot V^* = V^{-1} \cdot V^* \cdot H^* = V^{-1} \cdot V^* \cdot H^t. \tag{31}$$

One thus sees that the matrix $V^{-1} \cdot V^*$, which is a symmetric unitary matrix, is a solution of (27). However this matrix strongly depends on the parameters of H. From a statistical ensemble point of view this means that the ensemble of Hermitian matrices cannot be reduced to the ensemble of real Hermitian matrices with an independent Gaussian distribution for the entries in each case. The symmetric unitary matrix K we are looking for, has to be independent of the α_n and $\bar{\alpha}_n$ parameters.

4. Results

One question addressed in this paper is to decide whether or not the RMT analysis can detect 'higher genus integrability'. One should recall that the quantum Hamiltonian (1) exhibits genus zero integrability for the self-dual case ($\alpha_i = \overline{\alpha_i}$), or free fermion integrability for some algebraic conditions. In order to avoid these simple cases of integrability and stick to higher genus integrability, we choose to move, in the $\alpha_i, \overline{\alpha_i}$ parameter space, along a trajectory crossing, the integrable variety given by (2)–(5). In order to avoid the self-dual case, we choose $n \neq 1$ and fix r. From these values of r and n we deduce the values of $\alpha_1 = \alpha_3^\star$ and $\overline{\alpha_1} = \overline{\alpha_3}^\star$ and $\overline{\alpha_2}$ using the parametrization (7). The trajectory in the parameter space is obtained by varying α_2. In the following we will always consider the following trajectories:

$$\begin{aligned}
\alpha_1 &= \alpha_3^\star = \sqrt{1+r} + i\sqrt{1-r} & \alpha_2 &= t \\
\overline{\alpha_1} &= \overline{\alpha_3}^\star = \sqrt{n^2+rn} + i\sqrt{n^2-rn} & \overline{\alpha_2} &= n
\end{aligned} \tag{32}$$

where t, r and n are real parameters.

Integrability on this trajectory appears at the value $\alpha_2 = 1$. We concentrate on the value of the best β_{brody} deduced from (12) as a function of the parameter $t = \alpha_2$.

We have constructed the quantum Hamiltonian of the four-state Potts model for various chain sizes, up to eight ($L = 8$), i.e. matrices of size up to $4^8 \times 4^8 = 65\,536 \times 65\,536$. Since the size of the Hilbert space grows as 4^L, it is difficult to go much further. The results displayed below show that the size $L = 8$ is sufficient to answer the question we addressed. Using the complex characters and projectors associated with the group $Z_L \times Z_4$ (see (24)) we have performed the block diagonalization of the Hamiltonian. The dimensions of the $8 \times 4 = 32$ blocks are labelled by (e, c) which are respectively to the space index in (24) and the colour index in (24). The dimensions of the $8 \times 4 = 32$ blocks are gathered in table 1.

When L is a prime integer, the dimensions become simpler: all the blocks have the same dimensions $d_{\text{all}} = (4^L - 4)/4/L$ except the blocks of maximal symmetry with respect to the space group Z_L: $(e, c) = (0, c)$ which have dimension $d_{(0,c)} = 1 + d_{\text{all}}$.

We first found for each of the 32 blocks, that the eigenvalues are not degenerate in each block, and, furthermore, these blocks are irreducible. We then performed the unfolding in each
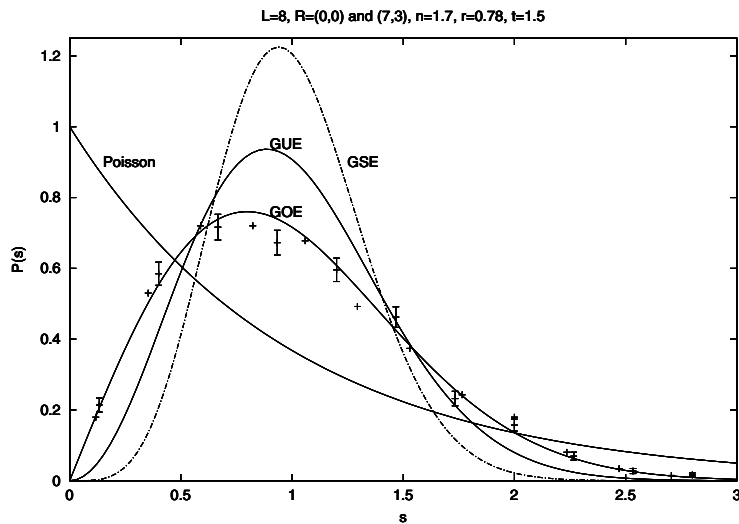
Figure 1. Level spacing distribution versus GOE, GUE, GSE and Poisson.

Table 1. Dimensions of the $8 \times 4 = 32$ blocks.

	$e = 0$	$e = 1$	$e = 2$	$e = 3$	$e = 4$	$e = 5$	$e = 6$	$e = 7$
$c = 0$	2070	2032	2060	2032	2066	2032	2060	2032
$c = 1$	2048	2048	2048	2048	2048	2048	2048	2048
$c = 2$	2064	2032	2064	2032	2064	2032	2064	2032
$c = 3$	2048	2048	2048	2048	2048	2048	2048	2048

block independently. All these calculations have been checked against full diagonalization for small sizes, as well as for special parameter sets yielding a real dihedral symmetry group. The behaviour in the various blocks is not significantly different. This is not totally surprising since the dimensions d_α of the various blocks are almost equal to the average dimension $d_\alpha \simeq 4^L/(4 \times L) = 2048$. Nevertheless, the statistics is better for larger blocks since the influence of the boundary of the spectrum and finite size effects are smaller. To get better statistics we have also averaged the results of several blocks for the same quantum chain size L. We moreover compared the four unfolding procedures, again getting similar results. We display the results on the largest size $L = 8$ for the best unfolding procedure, namely the Gaussian unfolding. Figure 1 shows two level spacing distributions $P(s)$, for, respectively, representation (0, 0) and representation (7, 3), for $r = 0.78, n = 1.7$, and $t = 1.5$, which correspond to $\alpha_1 = \alpha_3^\star = 1.334 + i0.469, \alpha_2 = 1.5, \overline{\alpha_1} = \overline{\alpha_3}^\star = 2.053 + i1.250$ and $\overline{\alpha_2} = 1.7$.

This figure clearly shows that the level spacing distribution is close to the GOE level spacing distribution. The GUE and GSE level spacing distributions are ruled out. Very similar results are obtained for the other blocks and for other values of the parameters away from the integrability value $\alpha_2 = t = 1$. We may compare the Brody and the GOE distributions at $r = 0.5, n = 2.1$, and $t = 1.5$, corresponding to $\alpha_1 = \alpha_3^\star = 1.225 + i0.707, \alpha_2 = t = 1.5, \overline{\alpha_1} = \overline{\alpha_3}^\star = 2.337 + i1.833$ and $\overline{\alpha_2} = 2.1$, for the block (0, 0). Figure 2 shows the level spacing distribution and the corresponding Brody fit (2.2) for the (least-squares) best value found to be $\beta_{\text{brody}} = 0.99$. On the same figure the GOE level spacing distribution is also displayed, both curves are almost indistinguishable.
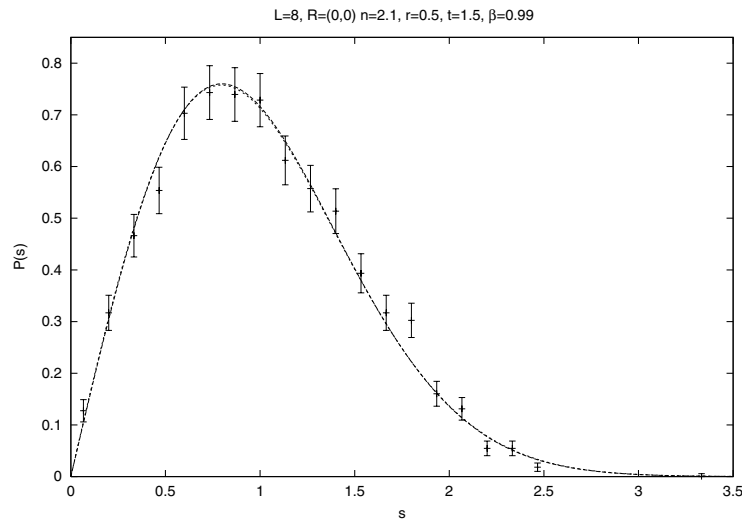
Figure 2. Level spacing distribution versus GOE distribution.
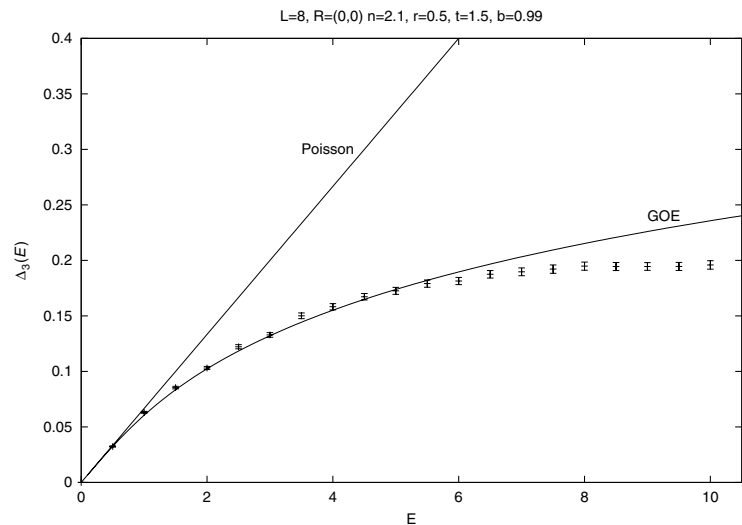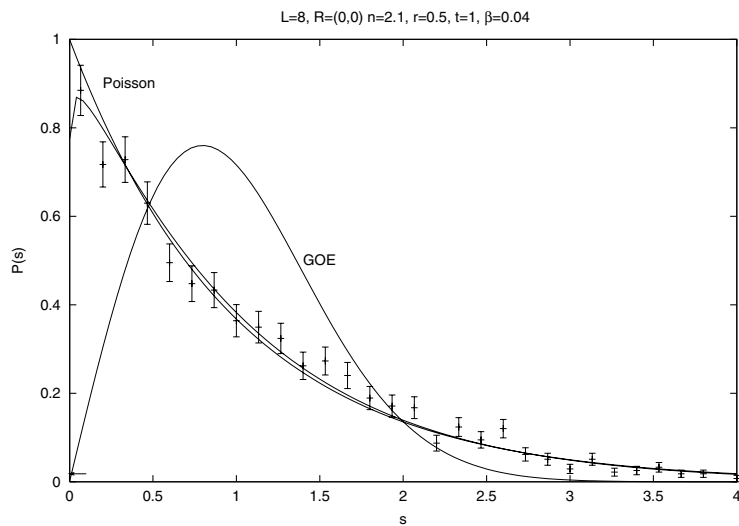

Figure 3. Spectral rigidity $\Delta_3(E)$ for $n = 2.1, t = 1$ versus spectral rigidity of the GOE.

As described in section 2 we can test how close we are to the GOE statistics, considering quantities such as the spectral rigidity $\Delta_3(E)$. This is depicted in figure 3 where the spectral rigidity for the same data as in figure 2 is compared with the spectral rigidity of the GOE together with the rigidity of random diagonal matrices (Poisson).

The agreement with the GOE rigidity is good up to a value of $E \simeq 6$, which means that the correlations involving up to six consecutive eigenvalues are properly taken into account by the GOE description.

Figures 4 and 5 display the level spacing distribution and the spectral rigidity for the integrable case $r = 0.5, n = 2.1$ and $t = 1$ which correspond to $\alpha_1 = \alpha_3^\star = 1.225 + \mathrm{i}0.707, \alpha_2 = t = 1, \overline{\alpha_1} = \overline{\alpha_3}^\star = 2.337 + \mathrm{i}1.833$ and $\overline{\alpha_2} = 2.1$.

L=8, R=(0,0) n=2.1, r=0.5, t=1, β=0.04

Figure 4. Level spacing distribution versus Poisson distribution.
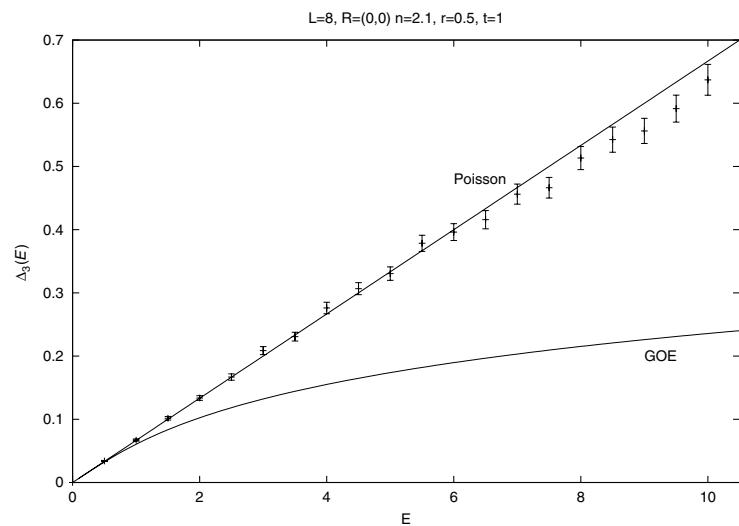
L=8, R=(0,0) n=2.1, r=0.5, t=1

Figure 5. Spectral rigidity $\Delta_3(E)$ for $n = 2.1, r = 0.5, t = 1$ versus Poissonian spectral rigidity.

Figure 4 shows the level spacing distribution compared to a Poisson distribution, and also compared to the GOE level spacing distribution. The best Brody distribution approximation of the data is found to be $\beta = 0.04$ using a least-squares fit. We have obtained very similar results with other values of the parameters n and r, *and for all the* 32 *blocks separately*, when t is kept equal to the (higher genus) integrability value $t = 1$. This extremely good agreement with a Poisson distribution is confirmed by the calculations of the spectral rigidity displayed in figure 5. The RMT analysis can therefore be used to detect integrability even when the integrability is not associated with Abelian curves. In other words the independence of eigenvalues (yielding the Poisson distribution) is not a consequence of the Abelian character of the algebraic varieties occurring in the Yang–Baxter equations.
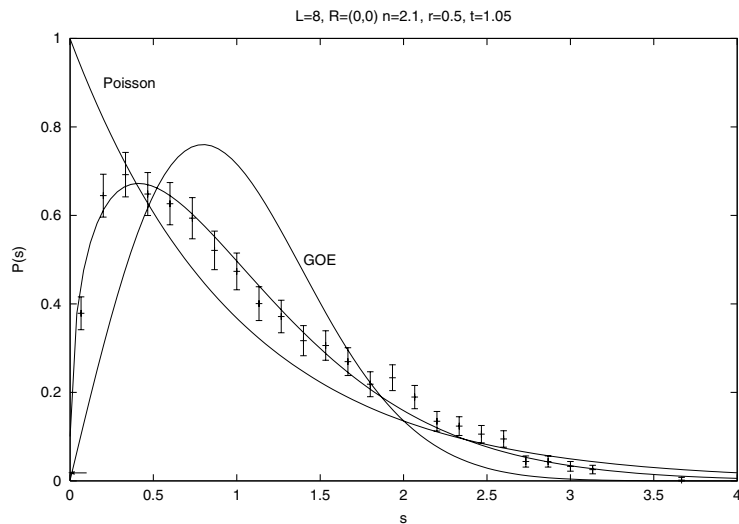
Figure 6. Level spacing distribution for $n = 2.1, r = 0.5, t = 1.05$ versus GOE distribution together with a Brody distribution for $\beta = 0.36$.

This extremely good agreement with an *independent eigenvalues* situation is found for $t = 1$ exactly. When t is slightly different from 1, the distribution is no longer Poissonian (as shown by figure 6) in agreement with the fact that the Poissonian distribution should appear only at the integrability value $t = 1$: as soon as t is no longer equal to 1, the independence of the eigenvalues is lost, and *eigenvalue repulsion sets in*. This is seen on the behaviour of $P(s)$ for small s. However, in the vicinity of $t = 1$, the full distribution is not exactly a Wigner distribution ($\beta_{brody} = 1$), and is an intermediate Brody distribution. We interpret this fact as a finite size effect. Figure 6 shows the level spacing distribution for exactly the same parameters as in figure 5 ($L = 8, r = 0.5, n = 2.1$, for the block $R = (0, 0)$) except parameter t which is changed into $t = 1.05$.

The best (least-squares) fitting parameter $\beta_{brody} = 0.36$. This intermediate value, between 0 and 1, is a consequence of the finite size of the quantum chain. One can certainly expect β_{brody} would tend, in the thermodynamic limit, to the GOE value $\beta_{brody} = 1$. In order to quantify this (finite size) transition from integrability to chaos, we calculate the best Brody parameter, as a function of the parameter t, keeping r and n constant. Figure 7 displays β_{brody}, as a function of t, for all the representations.

These results confirm a sharp transition from a GOE distribution to a Poisson distribution. In the thermodynamic limit one can expect β_{brody} to be equal to the GOE value $\beta_{brody} = 1$ for every value of the parameter t, except at point $t = 1$, where $\beta_{brody} = 0$.

To make this change of regime more intuitive, we also show, in figure 8, a window on the unfolded spectrum, as a function of parameter t, for $L = 7$. Only 25 unfolded eigenvalues are represented. One sees clearly, on the unfolded spectrum, the level repulsion for $t \neq 1$ and the level repulsion weakening around $t = 1$.

4.1. Discussion of the occurrence of GOE

The results presented above indicate a clear occurrence of a GOE distribution when $t \neq 1$. Numerically the previous results hold *for each of the 4L blocks*. This certainly requires
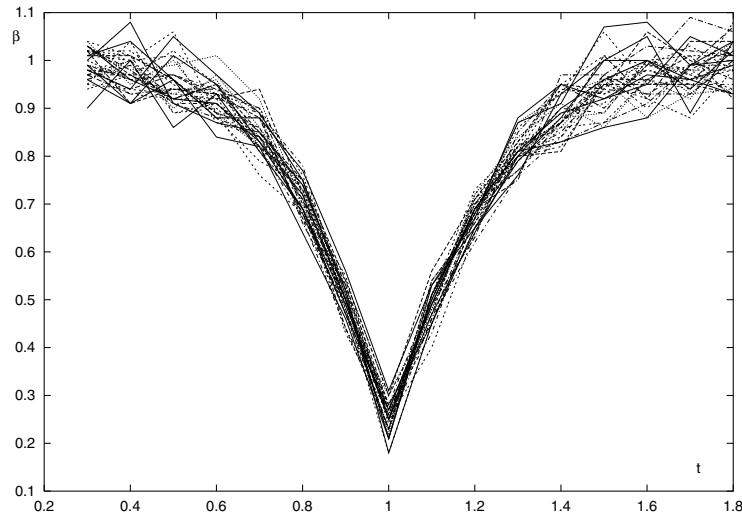
Figure 7. Best β_{brody} parameter as a function of parameter t for all the 32 representations.
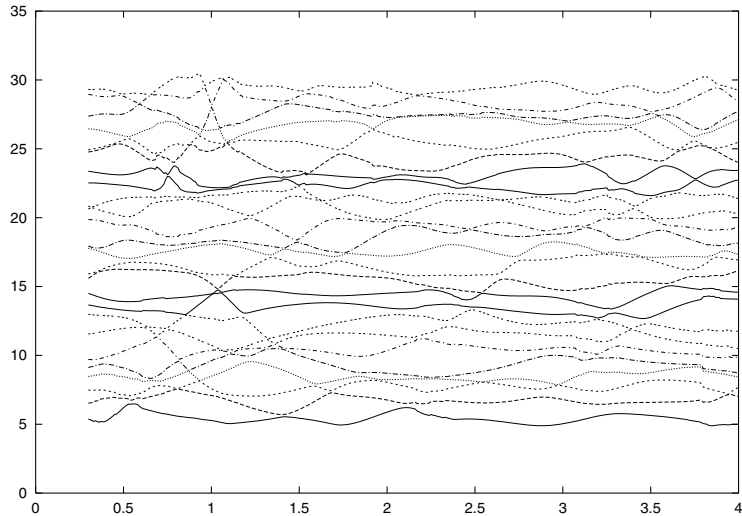

Figure 8. Window of the unfolded spectrum as a function of parameter t for seven sites. Twenty-five unfolded eigenvalues among $4^7 = 16\,384$ are given as a function of t.

Hamiltonian (1) to have additional symmetry properties compared to a generic Hermitian matrix. In the following we will see that a generalization of the time-reversal invariance property for the quantum Hamiltonian (1), namely condition (27) of section 3.3, seems to hold.

One can look for the matrix K of (27) in any basis, keeping in mind the particular transformation rule (29). If we examine form (22):

$$
\begin{aligned}
H_{ZXX} = H_Z + H_{XX} &= \left(H_Z + H_{XX}^{(s)} \right) + \alpha_{im} \cdot H_{XX}^{(as)} \\
&= H_{ZXX}^{(s)} + \alpha_{im} \cdot H_{XX}^{(as)} \qquad \text{with} \quad \alpha_{im} = \tfrac{1}{2}(\alpha_1 - \alpha_1^*) = \tfrac{1}{2}(\alpha_1 - \alpha_3)
\end{aligned} \tag{33}
$$

where $H_{XX}^{(s)}$ is a *real symmetric* matrix:

$$H_{XX}^{(s)} = -\sum_j \left[\frac{1}{2}(\alpha_1 + \alpha_3) \cdot (X_j X_{j+1}^\dagger + X_j^\dagger X_{j+1}) \right] - \sum_j \alpha_2 \cdot (X_j X_{j+1}^\dagger)^2 \quad (34)$$

and $H_{XX}^{(as)}$ is the *antisymmetric* matrix:

$$H_{XX}^{(as)} = -\sum_j [X_j X_{j+1}^\dagger - X_j^\dagger X_{j+1}]. \quad (35)$$

As a consequence of the hermiticity conditions, in particular $\overline{\alpha_1} = \overline{\alpha_3}^\star$ with $\overline{\alpha_2}$ real, H_Z is a real diagonal matrix. Thus, since $H_{XX}^{(s)}$ is real symmetric, $H_{ZXX}^{(s)}$ is also real symmetric. In other words, Hamiltonian (22) is real symmetric when $\alpha_{im} = 0$, in which case $K = K_R$ given by (20). *It is thus not surprising to see the occurrence of a GOE level spacing distribution on Hamiltonian* (1) *when $\alpha_1 = \alpha_3$ is real* (namely $r = 1$ with parametrization (7)).

When $\alpha_{im} \neq 0$, one looks for a matrix K, independent of the α_n and $\bar{\alpha}_n$, which commutes with $H_{ZXX}^{(s)}$ and anticommutes with $H_{XX}^{(as)}$.

The existence of K implies that the non-zero eigenvalues of $H_{XX}^{(as)}$ appear in opposite pairs, which we have checked up to size $L = 8$.

4.1.1. Small L cases. For $L = 3$, the symmetric unitary matrices K satisfying (27) are not simple tensor products[6], suggesting that we are not in a strict time-reversal invariance framework (see for instance equation (26.15), p 331 in [44]). For $L = 3$, the 64×64 matrices[7] K satisfying (27) are linear combinations of 12 quite simple involutive permutation matrices with entries equal to 0 or 1. For periodic boundary conditions, none of these linear combinations commute with S_{latt}, the lattice shift operator of one lattice shift spacing.

This non-trivial form of K is confirmed by its expression in the basis which block diagonalizes the Hamiltonian: the off-diagonal blocks $K_{\alpha,\beta}, \alpha \neq \beta$, of $K_{\text{block}} = P \cdot K \cdot P^t$ in (30) vanish and one can restrict condition (27) to each block $\alpha = (e, c)$, namely

$$H_\alpha \cdot K_{\alpha,\alpha} = K_{\alpha,\alpha} \cdot H_\alpha^t. \quad (36)$$

The off-diagonal blocks $K_{\alpha,\beta}$ also vanish for Hamiltonian (22), the unitary transformation (24) being replaced by P_{ZXX}.

For $L = 3$ the symmetry group is $Z_4 \times Z_3$, and there are $4 \times 3 = 12$ blocks $\alpha = (e, c)$, labelled in short by an index $0, 1, \ldots, 11$. The blocks $K_{\alpha,\alpha}$ can be written as

$$K_{\alpha,\alpha} = \lambda_\alpha \cdot k_{\alpha,\alpha} \quad (37)$$

where the $k_{\alpha,\alpha}$ are simple symmetric unitary matrices with as many entries as possible normalized to 1, and where the λ_α are complex numbers of unit modulus. The block matrices $k_{\alpha,\alpha}$ are given in appendix A.2 for Hamiltonian (1) or equivalently (22). For instance the block corresponding to the 'most symmetric' representation, namely $\alpha = (0, 0)$, reads

---

[6] Seeking for matrix $K = M \otimes M \otimes M$ satisfying (27) when $\alpha_{im} \neq 0$, one finds, from the commutation of K with H_Z, that M must be a symmetric matrix, and from the anticommutation of K with $H_{XX}^{(as)}$ that the only solution is the null matrix. Of course when $\alpha_{im} = 0$ one gets solution (20) taken for $L = 3$.

[7] If K_1 and K_2 are two unitary solutions of (27), $K_2 \cdot K_1^{-1}$ commutes with the family of H and $K_2^{-1} \cdot K_1$ commutes with the family of H^t. Thus the set of solutions of (27) is related to the set of matrices commuting with H.

for Hamiltonian (1) as well as for (22):

$$k_{0,0} = \begin{bmatrix} 1 & 0 & 0 & 0 & 0 & 0 \\ 0 & 0 & 0 & 1 & 0 & 0 \\ 0 & 0 & 1 & 0 & 0 & 0 \\ 0 & 1 & 0 & 0 & 0 & 0 \\ 0 & 0 & 0 & 0 & 1 & 0 \\ 0 & 0 & 0 & 0 & 0 & 1 \end{bmatrix}. \tag{38}$$

It is important to note that, up to the multiplicative (unit modulus) factors λ_α the blocks $k_{\alpha,\alpha}$ given in appendix A.2 are unique. This means that in each block α there exists *no non-trivial symmetry operator commuting with the family* (1) *of Hamiltonians H.*

$$[S_\alpha, H_\alpha] = 0 \qquad \forall \alpha_n, \overline{\alpha_n}, n = 1, 2, 3 \quad \Rightarrow S_\alpha = \text{Identity}. \tag{39}$$

For $L = 4$ we get similar results for Hamiltonian (22). The most symmetric block $(0, 0)$ yields a 20×20 involutive permutation matrix $k_{0,0}$. It is important to note that all blocks are quite similar to the ones described in appendix A.2 and are *unique up to multiplicative complex of unit modulus*. For $L = 4$, K is a 256×256 symmetric matrix. If one does not impose the unitarity condition, the set of all solutions of (27) reads

$$K = \sum_{n=0}^{n=15} p_n \cdot A_n \tag{40}$$

where the A_n are 256×256 symmetric matrices whose entries are equal to 0 except on at most one entry equal to one for each row or column. In contrast with the $L = 3$ case the A_n are singular matrices ($\det(A_n) = 0$), they are not permutation matrices. For certain choice of the parameters p_n one gets, from (40), a matrix K which is an symmetric real matrix with entries 0 or 1, representing an *involutive permutation* I_1.

Similar exact calculations of the blocks of matrix $P_{ZXX} \cdot K_{ZXX} \cdot P_{ZXX}^t$ have been performed for $L = 5$ and $L = 6$. Again one finds that the $\alpha \neq \beta$ off-diagonal blocks $K_{\alpha,\beta}$ vanish and that the $4L$ blocks $K_{\alpha,\alpha}$ are *unique up to multiplicative complex of unit modulus*.

As far as the $(0, 0)$ block is concerned one also finds that $k_{0,0}$ are (52×52 for $L = 5$ and 178×178 for $L = 6$) simple involutive permutation matrices.

All these results are detailed on a website [51] where the various blocks $k_{\alpha,\beta}$ are written for $L = 3$, $L = 4$, the blocks such that all the entries are 0 or 1 (but no root of unity) are given for $L = 5$, and $L = 6$ and furthermore the full 64×64 and 256×256 K matrices are written for $L = 3$ and 4.

For these values of L ($L = 3, 4, 5, 6$), the block matrices $k_{\alpha,\alpha}$ are remarkable matrices with entries 0, 1 or m-th *root of unity* ($m = 4L$).

4.1.2. Conjecture. It is difficult to describe all the $4L$ blocks $K_{\alpha,\alpha}$ ($\alpha \neq (0,0)$). It might be easier to describe the $4^L \times 4^L$ matrices K satisfying (27) without imposing the unitarity condition in a first step.

We conjecture that the solutions of (27) are linear combinations of $4L$ solutions which are involutive permutations I_n, *in the original basis* where X and Z are given by (16).

We conjecture moreover that the block diagonalization of H leads simultaneously to a block diagonalization of K into $4L$ blocks. The unitarity condition on K translates into a
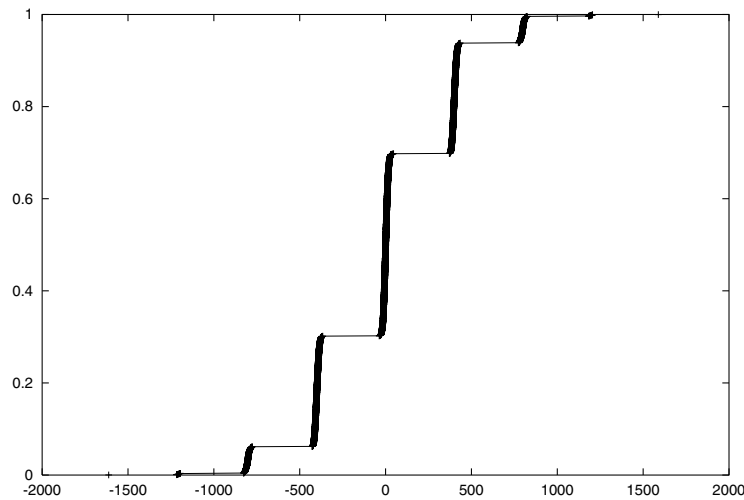
Figure 9. Integrated density of eigenvalues.

simple condition on a multiplicative factor for each block (modulus equal to one condition). The choice of these factors is the only indeterminacy.

4.1.3. Large α_{im} limit: deformation of a quantized spectrum still yielding GOE. It is difficult to find a simple closed expression for matrix K satisfying (27), for arbitrary L and α_{im}. We may examine the part $H_{XX}^{(as)}$ of the Hamiltonian and compare with the results of level spacing analysis of Hamiltonian (1) or (22) for large α_{im}.

Matrix $H_{XX}^{(as)}$ vanishes except on a set of rows and columns where its entries are equal to 0 or ± 1. Unfortunately the subspace corresponding to these rows and columns is not an invariant subspace of $H_{ZXX}^{(s)}$: $H_{XX}^{(as)}$ and $H_{ZXX}^{(s)}$ *do not commute*. Furthermore, this subspace becomes 'quite large' with increasing chain size L. Let us consider the dimension $d(L)$ of this subspace as a function of L. If $d(L)/4^L \to 0$ when $L \to \infty$ one could think that condition (27) 'tends to be verified' in the thermodynamic limit. In fact this is not the case: the ratio of $d(L)/4^L$ is a monotonic increasing function of L. For L running from $L = 3$ to 12, one gets the following values, for successive ratios of $d(L)/4^L$: 0.375, 0.406, . . . , 0.647, 0.663, 0.677.

More specifically, the antisymmetric matrix $H_{XX}^{(as)}$ has the same eigenvalues as the diagonal matrix H_{ZZ}^{im}:

$$H_{ZZ}^{im} = - \sum_j [Z_j Z_{j+1}^\dagger - Z_j^\dagger Z_{j+1}] \tag{41}$$

that is to say the relative integers $0, \pm 4, \pm 8, \pm 12, \ldots, \pm 4m$. For instance, for $L = 12$, one gets the eigenvalues $\pm 4, \pm 8, \pm 12, \pm 16, \pm 20, \pm 24$, respectively 3 920 928, 1 471 932, 268 752, 21 384, 528, four times.

We may go back to the level spacing distributions and rigidity calculations detailed in section 4, when α_{im} is large. This is an interesting situation where the spectrum of eigenvalues should be (up to the multiplicative factor α_{im}) a deformation of a set of integers $0, \pm 4, \pm 8, \pm 12, \ldots, \pm 4m$. Let us consider again $L = 8$ but for a large enough value of $\alpha_{im} = 200$. Figure 9 shows the integrated density of eigenvalues for $L = 8$. It is clear that the eigenvalues are (up to a multiplicative factor α_{im}) mainly located around the set of relative integers $0, \pm 4, \pm 8$.
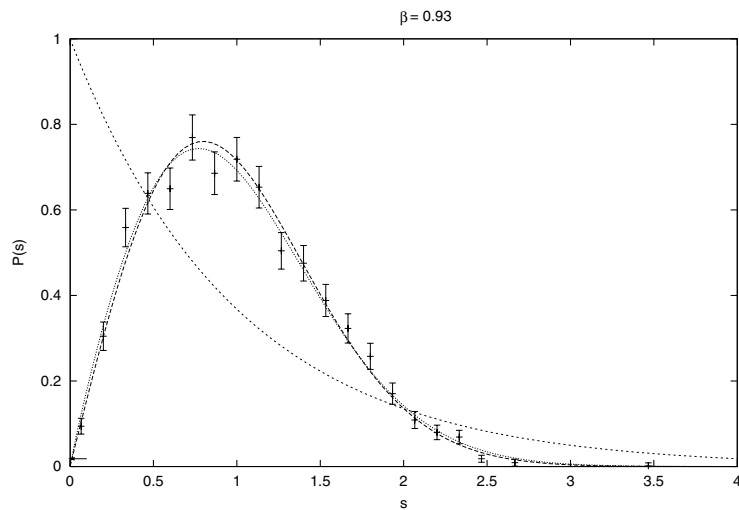
Figure 10. Level spacing distribution versus Poisson, GOE distributions and Brody distribution for $\beta_{\text{brody}} = 0.93$.

Figure 10 shows the corresponding level spacing distribution compared to the Poisson distribution, to the GOE distribution, and to the best (least-squares) fit by a Brody distribution. The agreement with a GOE statistics is extremely good since one gets $\beta_{\text{brody}} \simeq 0.93$.

Recalling the analysis which yields figures 3 and 5 in section 4, one also can perform rigidity calculations in this strong α_{im} limit. Similarly to the results displayed in figure 3, the rigidity analysis confirms, for each of the 32 representations, this GOE distribution. This is a non-trivial limit. This strong α_{im} limit yields a spectrum which is a *deformation of a spectrum of relative integers*. The unfolding procedure yields a level spacing distribution which is still GOE! It does not matter that the eigenvalues are concentrated near integers: what matters is the distribution of eigenvalues around these integers which still yields the universal GOE level spacing distribution.

This very good agreement is a strong indication of the GOE character of the level spacing distribution of the Hermitian Hamiltonian (1) in general.

4.2. Strategy for finding new integrable lattice models

One may use RMT analysis to find new integrable lattice models, which is extremely difficult analytically especially if they are associated with higher genus solutions of the Yang–Baxter equations.

It has been emphasized [24, 52, 53] that this type of integrability appears when the parameters verify very specific algebraic conditions: these conditions express that an infinite set of birational transformations degenerates into a *finite set* [52, 54–58]. We thus have a constructive way to find new possible integrability conditions [59]. However verifying that a particular subvariety of the parameter space of the model allows the Yang–Baxter (or the generalized star-triangle) relations to be satisfied, remains a very involved analytical task. The RMT analysis provides us with a numerically efficient way to verify if these algebraic subvarieties yield actual integrability conditions.

One can show that the general four-state classical two-dimensional chiral Potts model has a canonical elliptic parametrization. From this parametrization one may write down explicitly

the equations of these algebraic varieties, which are the only possible locations for the higher genus integrability conditions [50]. Various analyses, similar to the one summarized on figure 7, of β_{brody} as a function of parameter t, on various trajectories (7) in the parameter space of the quantum Hamiltonian (1), indicate that the integrable variety (2) is the only one with higher genus. Of course one cannot exclude the existence of higher codimension integrable varieties avoiding the trajectories (7) we have considered.

5. Conclusion

We have performed an RMT analysis of the quantum four-state Potts chain for different sizes of the quantum chain, and for different unfolding methods. Our calculations unambiguously exhibit a GOE statistics and exclude GUE (and GSE) statistics.

Our results indicate that there exists, for arbitrary size L, a symmetric unitary matrix K, such that $K \cdot H^t = H \cdot K$. This can be checked exactly for small lattice sizes $L = 2, 3, 4, 5, 6$. We conjecture that such a relation exists for all sizes of the chain, and for each of the $4L$ blocks (36). The existence of K would account for the statistics we find (GOE rather GUE).

When the Hamiltonian becomes integrable our analysis shows the change from the (generic) GOE distribution to a Poisson distribution and this reduction does not require the spectral curve to be of genus 0 or 1.

It is thus interesting to combine this RMT approach with more algebraic methods developed in previous publications [24, 52, 53]. These methods will give the algebraic subvarieties where a 'higher genus' integrability may appear, if any (the infinite set of these algebraic subvarieties can be obtained exactly for the four-state chiral Potts model [50]). As we have shown, the change in the level spacing statistics will signal integrability, bypassing the difficulties of the analytical approach.

Acknowledgments

Appendix

A.1. Generalized time-reversal invariance

The anti-unitary time-reversal operator T can be expressed as the product of a unitary operator K and the conjugation operator C, namely $T = K \cdot C$, where T is projectively an involution, namely $T^2 = \lambda.\text{Id}$, and where Id denotes the identity operator. The factor λ is equal to ± 1 as a consequence of the unitarity of K. The time-reversal operator T must change the time evolution operator according to

$$T \, e^{-iHt} T^{-1} = e^{+iHt} \tag{A.1}$$

or equivalently

$$T \, e^{-iHt} T = \lambda \cdot e^{+iHt}. \tag{A.2}$$

Expanding (A.1) or (A.2) in the time variable t one gets for every order n

$$K (H^\star)^n K^\star = \lambda \cdot H^n \qquad \forall n$$

yielding only two equations:

$$KK^\star = \lambda \tag{A.3}$$

$$KH^\star K^\star = \lambda \cdot H. \tag{A.4}$$

For a Hermitian Hamiltonian, (A.4) becomes, using (A.3):

$$H = K \cdot H^t \cdot K^{-1} \tag{A.5}$$

where H^t is the transpose of H. Since the operator K is a unitary one, (A.3) yields

$$K = \lambda.(K^\star)^{-1} = \lambda.K^t \tag{A.6}$$

where K^t denotes the transpose of K. Recalling that $\lambda = \pm 1$, we see, from (A.6), that K *must be either a symmetric or an antisymmetric unitary matrix.*

A.2. Matrix K as block diagonal matrices for L = 3 for Hamiltonian (22)

Let ω be the third root of unity: $\omega = -1/2 - \mathrm{i}\sqrt{3}/2$, and then consider the $L = 3$ case with $\alpha = 0, 1, 2, \ldots, 11$ indexing the twelve blocks defined in (37).

For Hamiltonian (22) and $K_{\mathrm{block}} = P_{ZXX} \cdot K_{ZXX} \cdot P_{ZXX}^t$ in (30), the off-diagonal blocks of K_{block} vanish and one finds the following expressions for the diagonal blocks $k_{\alpha,\alpha}$:

$$k_{3,3} = \begin{bmatrix} 1 & 0 & 0 & 0 & 0 & 0 \\ 0 & 0 & 1 & 0 & 0 & 0 \\ 0 & 1 & 0 & 0 & 0 & 0 \\ 0 & 0 & 0 & 1 & 0 & 0 \\ 0 & 0 & 0 & 0 & 1 & 0 \\ 0 & 0 & 0 & 0 & 0 & 1 \end{bmatrix} \qquad k_{6,6} = \begin{bmatrix} 1 & 0 & 0 & 0 & 0 & 0 \\ 0 & 1 & 0 & 0 & 0 & 0 \\ 0 & 0 & 1 & 0 & 0 & 0 \\ 0 & 0 & 0 & 0 & 1 & 0 \\ 0 & 0 & 0 & 1 & 0 & 0 \\ 0 & 0 & 0 & 0 & 0 & 1 \end{bmatrix}$$

$$k_{1,1} = \begin{bmatrix} 0 & 0 & 1 & 0 & 0 \\ 0 & 1 & 0 & 0 & 0 \\ 1 & 0 & 0 & 0 & 0 \\ 0 & 0 & 0 & \omega & 0 \\ 0 & 0 & 0 & 0 & 1 \end{bmatrix} \qquad k_{4,4} = \begin{bmatrix} \omega & 0 & 0 & 0 & 0 \\ 0 & 0 & 1 & 0 & 0 \\ 0 & 1 & 0 & 0 & 0 \\ 0 & 0 & 0 & \omega & 0 \\ 0 & 0 & 0 & 0 & 1 \end{bmatrix},$$

$$k_{7,7} = \begin{bmatrix} \omega & 0 & 0 & 0 & 0 \\ 0 & 1 & 0 & 0 & 0 \\ 0 & 0 & 1 & 0 & 0 \\ 0 & 0 & 0 & 0 & 1 \\ 0 & 0 & 0 & 1 & 0 \end{bmatrix} \qquad k_{10,10} = \begin{bmatrix} \omega & 0 & 0 & 0 & 0 \\ 0 & 0 & 1 & 0 & 0 \\ 0 & 1 & 0 & 0 & 0 \\ 0 & 0 & 0 & 1 & 0 \\ 0 & 0 & 0 & 0 & \omega \end{bmatrix}$$

and $k_{9,9} = k_{3,3}$, the block $k_{0,0}$ *is the same as the one for Hamiltonian* (1). Furthermore, $k_{2,2}$ is equal to block $k_{1,1}$ where ω is changed into ω^2, i.e. $k_{2,2}(\omega) = k_{1,1}(\omega^2)$. Similarly one gets $k_{5,5}(\omega) = k_{4,4}(\omega^2)$ as well as $k_{8,8}(\omega) = k_{7,7}(\omega^2)$ and $k_{11,11}(\omega) = k_{10,10}(\omega^2)$.

References

[1] Rosenzweig N and Porter C E 1960 *Phys. Rev.* **120** 1698
[2] Gutzwiller M C 1990 *Chaos in Classical and Quantum Mechanics (Interdisciplinary Applied Mathematics)* (Berlin: Springer)

[3] Wigner E P 1955 *Ann. Math.* **62** 548
    Wigner E P 1957 *Ann. Math.* **65** 203
    Wigner E P 1958 *Ann. Math.* **67** 325
[4] Dyson F J 1962 *J. Math. Phys.* **3** 140
    Dyson F J 1962 *J. Math. Phys.* **3** 157
    Dyson F J 1962 *J. Math. Phys.* **3** 166
[5] Mehta M L 1991 *Random Matrices* 2nd edn (San Diego, CA: Academic)
[6] Fan C and Wu F Y 1970 *Phys. Rev.* B **3** 723
[7] Felderhof B U 1973 *Physica* **66** 509
[8] Bohigas O 1991 *Les Houches, 1989, Chaos et Physique Quantique* ed M-J Giannoni *et al* (Amsterdam: North Holland)
[9] Meyer H, Anglès d'Auriac J-C and Maillard J-M 1997 *Phys. Rev.* E **55** 5380
[10] Jaekel M T and Maillard J M 1985 *J. Phys. A: Math. Gen.* **18** 1229
[11] Georges A, Hansel D, Le Doussal P and Maillard J-M 1987 *J. Phys. A: Math. Gen.* **20** 5299
[12] Kasteleyn P W 1974 Exactly solvable lattice models *Proc. 1974 Wageningen Summer School: Fundamental Problems in Statistical Mechanics III* ed E G D Cohen (Amsterdam: North-Holland) pp 103–55
[13] Sutherland B 1970 *J. Math. Phys.* **11** 3183
[14] Gaudin M 1983 *La fonction d'onde de Bethe (Collection du CEA Série Scientifique)* (Paris: Masson)
[15] Lieb E H and Wu F Y 1972 *Phase Transitions and Critical Phenomena* vol 1 ed C Domb and M Green (New York: Academic) pp 331–49
[16] Baxter R 1982 *Exactly Solved Models in Statistical Mechanics* (New York: Academic)
[17] Baxter R J, Perk J H H and Au-Yang H 1988 *Phys. Lett.* A **128** 138
[18] Au-Yang H, McCoy B M, Perk J H H, Tang S and Yan M-L 1987 *Phys. Lett.* A **123** 219
[19] Howes S, Kadano L P and den Nijs M 1983 *Nucl. Phys.* B **215** 169
[20] von Gehlen G and Rittenberg V 1985 *Nucl. Phys.* B **257** 351
[21] Dolan L and Grady M 1982 *Phys. Rev.* D **25** 1587
[22] Dasmahapatra S, Dedem R, Klassen T R, McCoy B M and Melzer E 1993 Quasi-particles, conformal field theory and q-series *Yang–Baxter Equations in Paris* ed J-M Maillard (Singapore: World Scientific)
[23] Albertini G 1993 Exact spectrum of the 3-state Potts chain *Yang–Baxter Equations in Paris* ed J-M Maillard (Singapore: World Scientific)
[24] Bellon M, Maillard J-M and Viallet C-M 1992 *Phys. Lett.* B **281** 315
[25] Bruus H and Anglès d'Auriac J-C 1996 *Europhys. Lett.* **35** 321
[26] Hsu T C and Anglès d'Auriac J-C 1993 *Phys. Rev.* B **47** 14291
[27] Meyer H, Anglès d'Auriac J-C and Bruus H 1996 *J. Phys. A: Math. Gen.* **29** L483
[28] Meyer H 1996 *PhD Thesis* Univ. J Fourier, Grenoble, France
[29] Dupuis N and Montambaux G 1991 Aharonov–Bohm flux and statistics of energy levels in metals *Phys. Rev.* B **43** 14 390
[30] Poilblanc D, Ziman T, Bellisard J, Mila F and Montambaux G 1993 *Europhys. Lett.* **22** 537
[31] Robnik M and Berry M V 1986 *J. Phys. A: Math. Gen.* **19** 669
[32] Jimbo M, Miwa T, Mori Y and Sato M 1980 *Physica* D **1** 80–158
[33] Tracy C A and Widom H 1994 *Commun. Math. Phys.* **163** 33–72
[34] Forrester P J and Witte N S 2002 Application of the τ-function theory of Painlevè equations to random matrices: P_V, P_{III}, the LUE, JUE and CUE *Preprint* arXiv:math-ph/0201051
[35] Forrester P J and Witte N S 2002 τ-function evaluation of gap probabilities in orthogonal and symplectic matrix ensembles *Preprint* arXiv:math-ph/0203049
[36] Forrester P J and Witte N S 2002 Application of the τ-function theory of Painlevè equations to random matrices: P_{VI}, the JUE, CyUE, cJUE and scaled limits *Preprint* arXiv:math-ph/0204008
[37] Montambaux G, Poilblanc D, Bellisard J and Sire C 1993 *Phys. Rev. Lett.* **70** 497
[38] van Ede, van der Pals and Gaspard P 1994 *Phys. Rev.* E **49** 79
[39] Bruus H and Anglès d'Auriac 1996 *Preprint* cond-mat/9610142
    Bruus H and Anglès d'Auriac J-C 1997 *Phys. Rev.* B **55** 9142
[40] Bashilov Y A and Pokrovsky S V 1980 *Commun. Math. Phys.* **76** 129
[41] Marcu M, Regev A and Rittenberg V 1981 *J. Math. Phys.* **22** 2740
[42] Anglès d'Auriac J C and Iglòi F 1998 *Phys. Rev.* E **58** 241
[43] Lapack Library webpage http://www.netlib.org/lapack
[44] Wigner E P 1959 *Group Theory and Its Application to the Quantum Mechanics of Atomic Spectra* (New York: Academic)
[45] Weyl H 1946 *Classical Groups* (Princeton, NJ: Princeton University Press)

[46] Chevalley C 1946 *Theory of Lie Groups* (Princeton, NJ: Princeton University Press) pp 16–24
[47] Dieudonné J-A 1955 *La Géométrie des Groupes Classiques (Ergeb. d. Math. vol 5)* (Berlin: Springer)
[48] von Gehlen G 1991 *J. Phys. A: Math. Gen.* **24** 5371
[49] von Gehlen G 1994 *Int. J. Mod. Phys.* B **8** 3507
[50] Anglès d'Auriac J-C, Maillard J-M and Viallet C M in preparation
[51] Webpage http://crtbt.polycnrs-gre.fr/theo/pagesperso/dauriac/QPOTTS/QPotts.html
[52] Maillard J-M 1986 *J. Math. Phys.* **27** 2776
[53] Bellon M P, Maillard J-M and Viallet C-M 1991 *Phys. Lett.* B **260** 87
[54] Jaekel M T and Maillard J-M 1985 *J. Phys. A: Math. Gen.* **18** 1229
[55] Maillard J-M and Rollet G 1994 *J. Phys. A: Math. Gen.* **27** 6963
[56] Meyer H, Anglès d'Auriac J-C, Maillard J-M and Rollet G 1994 *Physica* A **208** 223
[57] Hansel D and Maillard J-M 1988 *Phys. Lett.* A **133** 11
[58] Maillard J-M and Rammal R 1983 *J. Phys.* A **16** 353
[59] Boukraa S and Maillard J-M 2001 *J. Stat. Phys.* **102** 641